Identification and Characterization of an Essential Family of Inositol Polyphosphate 5-Phosphatases (*INP51*, *INP52* and *INP53* Gene Products) in the Yeast *Saccharomyces cerevisiae*

Leslie E. Stolz,* Chau V. Huynh,† Jeremy Thorner,† and John D. York*

**Department of Pharmacology and Cancer Biology and Department of Biochemistry, Duke University Medical Center, Durham, North Carolina27710, and †Department of Molecular and Cell Biology, Division of Biochemistry and Molecular Biology, University of California, Berkeley, California 94720-3202*

Manuscript received October 17, 1997
Accepted for publication December 16, 1997

ABSTRACT

We recently demonstrated that the *S. cerevisiae INP51* locus (YIL002c) encodes an inositol polyphosphate 5-phosphatase. Here we describe two related yeast loci, *INP52* (YNL106c) and *INP53* (YOR109w). Like Inp51p, the primary structures of Inp52p and Inp53p resemble the mammalian synaptic vesicle-associated protein, synaptojanin, and contain a carboxy-terminal catalytic domain and an amino-terminal *SAC1*-like segment. Inp51p (108 kD), Inp52p (136 kD) and Inp53p (124 kD) are membrane-associated. Single null mutants (*inp51*, *inp52*, or *inp53*) are viable. Both *inp51 inp52* and *inp52 inp53* double mutants display compromised cell growth, whereas an *inp51 inp53* double mutant does not. An *inp51 inp52 inp53* triple mutant is inviable on standard medium, but can grow weakly on media supplemented with an osmotic stabilizer (1 M sorbitol). An *inp51* mutation, and to a lesser degree an *inp52* mutation, confers cold-resistant growth in a strain background that cannot grow at temperatures below 15°. Analysis of inositol metabolites *in vivo* showed measurable accumulation of phosphatidylinositol 4,5-*bis*phosphate in the *inp51* mutant. Electron microscopy revealed plasma membrane invaginations and cell wall thickening in double mutants and the triple mutant grown in sorbitol-containing medium. A fluorescent dye that detects endocytic and vacuolar membranes suggests that the vacuole is highly fragmented in *inp51 inp52* double mutants. Our observations indicate that Inp51p, Inp52p, and Inp53p have distinct functions and that substrates and/or products of inositol polyphosphate 5-phosphatases may have roles in vesicle trafficking, membrane structure, and/or cell wall formation.

UPON agonist stimulation of mammalian cells, phospholipase C hydrolyzes phosphatidylinositol 4,5-*bis*phosphate (PtdIns[4,5]P_2) to produce the second messengers, inositol 1,4,5-*tris*phosphate (Ins[1,4,5]P_3) and diacylglycerol. Diacylglycerol activates protein kinase C, while Ins[1,4,5]P_3 mobilizes intracellular Ca^{2+} (reviewed in Bansal and Majerus 1990; Berridge 1993; Hokin 1985; Majerus 1992; Majerus *et al.* 1990). Inositol polyphosphate 3-kinases can convert Ins[1,4,5]P_3 to Ins[1,3,4,5]P_4 (Irvine *et al.* 1988) and phosphatidylinositol 3-kinases can convert PtdIns[4,5]P_2 to PtdIns-[3,4,5]P_3 (Hawkins *et al.* 1992; Irvine *et al.* 1988). Evidence indicates that PtdIns[4,5]P_2 and PtdIns[3,4,5]P_3, and their derivatives, play roles in numerous cellular processes, including secretion regulation (Hay *et al.* 1995) and modulation of the actin cytoskeleton (Hartwig *et al.* 1995; Janmey *et al.* 1992). Additionally, certain protein structural elements, including Src-homology-2 (SH2), pleckstrin homology (PH), and phosphotyrosine-binding (PTB) motifs, can bind both soluble and lipid-linked inositol polyphosphates (Harlan *et al.* 1994; Rameh *et al.* 1995; Zhou *et al.* 1995). Hence, the physiological effects of these compounds may be mediated by direct association with certain target proteins rather than by indirect effects on the biophysical properties of membranes.

A balance of kinase, phosphatase, and phospholipase activities regulates the cellular level of these soluble and lipid-linked inositol phosphates. These activities include the inositol polyphosphate 5-phosphatase (hereafter 5-Ptase) family (reviewed in Drayer *et al.* 1996; Irvine 1992; Majerus 1996; Mitchell *et al.* 1996). The 5-Ptases are Mg^{2+}-dependent enzymes that remove the phosphoryl moiety from the C5 position of the inositol ring in inositol polyphosphate compounds. These enzymes were first identified based on their ability to terminate Ins[1,4,5]P_3-mediated Ca^{2+} release, since the product, Ins[1,4]P_2, is unable to mobilize Ca^{2+} (Connolly *et al.* 1985). To date, at least ten mammalian 5-Ptases have been identified. One hallmark of a 5-Ptase is the presence of two consensus sequences, WXGDXN(Y/F)R and P(A/S)W(C/T)DRIL (Jefferson and Majerus 1995). Mutational analysis demonstrates that these residues participate in substrate binding and/or catalysis (Communi and Erneux 1996; Communi *et al.* 1996; Jefferson and Majerus 1996).

The 5-Ptases are classified into four groups, based

Corresponding author: John D. York, Department of Pharmacology and Cancer Biology, Duke University Medical Center, DUMC 3813, Durham, NC 27710. E-mail: yorkj@acpub.duke.edu

mainly on substrate specificity (Jefferson *et al.* 1997). Type I enzymes act only on the soluble inositol polyphosphates Ins[1,4,5]P_3 and Ins[1,3,4,5]P_4. Type I 5-Ptases have been cloned and characterized from a number of tissues (Connolly *et al.* 1985; De Smedt *et al.* 1994; De Smedt *et al.* 1996; Laxminarayan *et al.* 1993; Laxminarayan *et al.* 1994; Verjans *et al.* 1994). These enzymes are thought to be responsible for termination of Ins[1,4,5]P_3-induced Ca^{2+} mobilization.

Type II enzymes can hydrolyze both Ins[1,4,5]P_3 and Ins[1,3,4,5]P_4, as well as PtdIns[4,5]P_2 and PtdIns[3,4,5]P_3 (Jackson *et al.* 1995; Matzaris *et al.* 1994). The first member of this class was identified in platelets (Jefferson and Majerus 1995; Mitchell *et al.* 1989); however, other isoforms have been identified in other tissues (Palmer *et al.* 1994; Woscholski *et al.* 1995). This subfamily contains the Golgi-asssociated 5-Ptase OCRL-1 (Olivos-Glander *et al.* 1995), which is defective in patients with oculocerebrorenal, or Lowe's, syndrome (Attree *et al.* 1992). Another type II enzyme is the neuronal protein, synaptojanin, which is involved in synaptic vesicle recycling (McPherson *et al.* 1994a,b; McPherson *et al.* 1996). The N terminus of synaptojanin is homologous to *S. cerevisiae* Sac1p. The *SAC1* gene was first identified as a suppressor of certain temperature-sensitive actin alleles (Novick *et al.* 1989). Since then, Sac1p has been implicated in phospholipid metabolism, vesicle-actin cytoskeleton interaction, and secretory transport (Cleves *et al.* 1989; Kearns *et al.* 1997; Mayinger *et al.* 1995; Whitters *et al.* 1993).

Type III 5-Ptases only hydrolyze PtdIns[3,4,5]P_3 and are associated with PtdIns 3-kinase (Jackson *et al.* 1995). Finally, type IV 5-Ptases, which include the protein SHIP and its alternative splice variants, SIP-110, SIP-130, and SIP-145 (Damen *et al.* 1996; Lioubin *et al.* 1996) are associated with tyrosine-phosphorylated growth factor receptors (Jefferson *et al.* 1997). These enzymes can hydrolyze both PtdIns[3,4,5]P_3 and Ins[1,3,4,5]P_4.

It remains unclear why so many different 5-Ptases exist. However, the importance of these enzymes is demonstrated by examination of the *S. cerevisiae* genome sequence which revealed the presence of an open reading frame, which we designated *INP51*, that bears striking similarity to the synaptojanin subclass of 5-Ptases. Detailed characterization of *INP51* is presented elsewhere (L. E. Stolz, W. J. Kuo, J. Longchamps, M. K. Sekhon, and J. D. York, unpublished results). With the completion of the entire *S. cerevisiae* genome, however, we found two additional open reading frames, designated *INP52* and *INP53*, that are highly homologous to *INP51*. We demonstrate here that these two loci encode functional proteins of the predicted molecular weight. In addition, we describe the growth properties, biochemical consequences, and morphological perturbations that result from mutations in *INP51*, *INP52*, and *INP53*, alone and in combination. We show that these three genes comprise an essential gene family and provide additional insights about the potential cellular functions of these enzymes.

MATERIALS AND METHODS

Strains, media, and genetic methods: Yeast strains used in this study are listed in Table 1. The cells were propagated in standard rich (YPD) medium, or in complete minimal medium (CM) lacking the appropriate nutrient(s) to maintain selection for plasmids or markers. Standard procedures for yeast genetic manipulations were used (Ausubel *et al.* 1995; Guthrie and Fink 1991). The ability of a given yeast strain to propagate at 12° was assessed by dispersing single cells on a YPD plate using a micromanipulator and, after incubation for an appropriate amount of time, observing the growth under a microscope.

Gene disruption and strain construction: *INP51* was disrupted and replaced with the *LEU2* gene as described elsewhere (L. E. Stolz, W. J. Kuo, J. Longchamps, M. K. Sekhon, and J. D. York, unpublished results). The entire open reading frame of *INP52* was disrupted and replaced with *HIS3* as follows. *HIS3* was amplified from pRS303 (Sikorski and Heiter 1989) by PCR with the sense primer 5′-CGAAACAGCAAACTAGAAAGATAGCAATAGTTTCAGAAACACATGGCAGATTGTACTGAGAGTGC-3′ and the antisense primer 5′-GTGGAGGCCTTTGCTGGCTCAGGATCTTCTGTAGTGGACACACCTCCTTACGCATCTGTGCGG-3′ (where the underlined bases correspond to the *INP52* coding sequence and the remainder of the primer is common to the pRS series of plasmids) under reaction conditions recommended by the Taq polymerase manufacturer (Boehringer Mannheim Corp., Indianapolis). The resulting *inp52::HIS3* PCR product was used for DNA-mediated transformation of strain W303 (*MAT***a**/*MAT*α) using the standard lithium acetate protocol (Ausubel *et al.* 1995). Stable His^+ transformants were selected on $^-$His plates and verified by PCR of the genomic DNA using a sense primer complementary to the chromosomal region 5′ of the *INP52* locus (5′-GGTCGAAGGTAAGAATGCTGCGGC-3′) and an antisense primer corresponding to a sequence in *HIS3* (5′-GCCTCATCCAAAGGCGC-3′). Heterozygous *inp52::HIS3*/*INP52* transformants were sporulated on 0.3% potassium acetate plates (Guthrie and Fink 1991). The resulting tetrads were dissected onto YPD plates, then replica-plated onto $^-$His plates to identify haploid spores carrying the *inp52::HIS3* allele. These *inp52::HIS3* spores were again verified by both PCR, as above, and immunoblotting cell extracts (see below) to confirm the absence of the *INP52*-encoded polypeptide.

The entire *INP53* open reading frame was also disrupted and replaced with the *HIS3* gene as described above, except that the template providing *HIS3* was plasmid pJJ217 (Jones and Prakash 1990), the sense primer was 5′-AGAAAATAACTGGGGCGAAGAATATCTAGTTATCCACTCCTTCATAGAGCCTCCTCTAGTACACTC-3′, and the antisense primer was 5′-AAAGGGATACAAACGGAACAACAACCACACTTCAAAGATAACATATTCGCGCGCCTCGTTCAGAAT-3′ (where the underlined bases correspond to the *INP53* coding sequence and the remainder correspond to sequences in pJJ217). The resulting *inp53::HIS3* PCR product was transformed as above, and His^+ transformants were selected and verified by PCR, as described above, except that the sense primer for amplification of genomic DNA from candidate transformants was complementary to the chromosomal region on the 5′-side of the *INP53* locus (5′-TAGGGATTTTTCGAGCACTACTGC-3′). Heterozygous *inp53::HIS3*/*INP53* diploids were sporulated and dissected as above. Haploid spores carrying the *inp53::HIS3* allele were verified by both PCR, as above, and

TABLE 1

Yeast strains used in this study

Strain	Genotype	Reference
W303	*MAT***a**/*MAT*α *ade2-1/ade2-1 ura3-1/ura3-1 his3-11,15/his3-11,15 trp1-1/trp1-1 leu2-3,112/leu2-3,112 can1-100/can1-100*	[a]
JYY3	*MAT***a** *ade2-1 ura3-1 his3-11,15 trp1-1 leu2-3,112 can1-100 inp51::LEU2*	Stolz *et al.* 1997
JYY4	*MAT*α *ade2-1 ura3-1 his3-11,15 trp1-1 leu2-3,112 can1-100 inp51::LEU2*	Stolz *et al.* 1997
LSY66	*MAT***a** *ade2-1 ura3-1 his3-11,15 trp1-1 leu2-3,112 can1-100 inp52::HIS3*	This study
LSY67	*MAT*α *ade2-1 ura3-1 his3-11,15 trp1-1 leu2-3,112 can1-100 inp52::HIS3*	This study
LSY75	*MAT*α *ade2-1 ura3-1 his3-11,15 trp1-1 leu2-3,112 can1-100 inp53:HIS3*	This study
LSY76	*MAT***a** *ade2-1 ura3-1 his3-11,15 trp1-1 leu2-3,112 can1-100 inp53::HIS3*	This study
LSY69	*MAT*α *ade2-1 ura3-1 his3-11,15 trp1-1 leu2-3,112 can1-100 inp51::LEU2*	This study
LSY70	*MAT***a** *ade2-1 ura3-1 his3-11,15 trp1-1 leu2-3,112 can1-100 inp51::LEU2 inp52:HIS3*	This study
LSY103	*MAT***a** *ade2-1 ura3-1 his3-11,15 trp1-1 leu2-3,112 can1-100 inp51::LEU2 inp53::HIS3*	This study
LSY105	*MAT***α** *ade2-1 ura3-1 his3-11,15 trp1-1 leu2-3,112 can1-100 inp51::LEU2 inp53::HIS3*	This study
LSY176	*MAT*α *ade2-1 ura3-1 his3-11,15 trp1-1 leu2-3,112 can1-100 inp52::HIS3 inp53::HIS3*	This study
LSY178	*MAT***a** *ade2-1 ura3-1 his3-11,15 trp1-1 leu2-3,112 can1-100 inp52::HIS3 inp53::HIS3*	This study
LSY94	*MAT*α *ade2-1 ura3-1 his3-11,15 trp1-1 leu2-3,112 can1-100 inp51::LEU2 inp52::HIS3 inp53::HIS3 pRSINP51*	This study
LSY98	*MAT***a** *ade2-1 ura3-1 his3-11,15 trp1-1 leu2-3,112 can1-100 inp51::LEU2 inp52::HIS3 inp53::HIS3 pRSINP51*	This study
LSY193	*MAT***a**/*MAT*α *ade2-1/ade2-1 ura3-1/ura3-1 his3-11,15/his3-11,15 trp1-1/trp1-1 leu2-3,112/leu2-3,112 can1-100/can1-100 inp51::LEU2/INP51 inp52::HIS3/INP52 inp53::HIS3/INP53*	This study

[a] Strain W303 was kindly provided by S. Wente (Washington University, St. Louis).

immunoblotting of cell extracts (see below) to confirm the absence of the *INP53* encoded polypeptide.

To construct *inp51 inp52* and *inp51 inp53* double mutants, haploid cells carrying the *inp51::LEU2* allele were mated with cells of opposite mating type containing either the *inp52::HIS3* allele or the *inp53::HIS3* allele. The diploids were sporulated and dissected, then replica plated onto selective media to determine haploid double knockouts, which were verified one more time with PCR. To construct the *inp52 inp53* double mutant, a haploid cell carrying the *inp52::HIS3* allele was mated with a haploid cell of the opposite mating type carrying the *inp53::HIS3* allele. The His^+ spores were verified as double mutants by PCR.

To construct the *inp51 inp52 inp53* triple mutant, a haploid *inp51::LEU2 inp52::HIS3* double mutant was mated with a haploid *inp53::HIS3* of the opposite mating type. Upon sporulation of the resulting diploid on normal medium, no nonparental ditype tetrads were found in which His^+:His^- segregrated 2:2 and cosegregated with Leu^+, indicating that the triple mutation is lethal. To verify that the triple mutant is inviable, we introduced into the *inp51::LEU2/INP51 inp52::HIS3/INP52 inp53::HIS3/INP53* diploid strain a plasmid, designated pRS*INP51* (L. E. Stolz, W. J. Kuo, J. Longchamps, M. K. Sekhon, and J. D. York, unpublished results), which carries the wild-type *INP51* gene driven by its endogenous promoter in the *URA3*-containing *CEN* vector, pRS316 (Sikorski and Heiter 1989). Upon sporulation and dissection, nonparental ditype tetrads were obtained in which His^+:His^- segregrated 2:2 and cosegregated with Leu^+ and Ura^+. To confirm that the Leu^+ His^+ Ura^+ spores represented authentic triple mutants, their inability to grow on CM plates containing 1 mg/ml 5-fluoroorotic acid (5-FOA) was tested.

Immunoblot analysis: Protein extracts were prepared from yeast strains by lysis of spheroplasts (Ausubel *et al.* 1995). Briefly, cells were grown in YPD to a density of 3×10^7 cells/ml, harvested by centrifugation, washed with ice-cold H_2O, resuspended at 3×10^8 cells/ml in Z buffer (1 M sorbitol, 10 mm $MgCl_2$, 50 mm Na-HEPES, pH 7.5) containing 30 mm dithiothreitol (DTT), incubated with gentle agitation on a rocker platform for 15 min at room temperature, collected by centrifugation, resuspended in Z buffer containing 1 mm DTT and 5 mg/ml Zymolyase 20T (Seikagaku Corp., Tokyo, Japan), and incubated for an additional 40 min with gentle agitation at room temperature. The resulting spheroplasts were collected by centrifugation, washed twice with Z buffer containing 1 mm DTT, and resuspended in 100 μl ice-cold lysis buffer (1 mm EGTA, 5 mm $MgCl_2$, 50 mm Na-HEPES, pH 7.5) containing 1 mm phenylmethylsulfonyl fluoride (PMSF). The suspension was subjected to sonic irradiation for 20 sec on ice, then the resulting crude lysate was separated into soluble and particulate fractions by centrifugation at 20,000 $\times$ *g* for 5 min. The pellet fraction was resuspended in 100 μl fresh lysis buffer and homogenized by brief sonication.

Soluble and particulate fractions were diluted in 2× sodium dodecyl sulfate (SDS) gel sample buffer, resolved by electrophoresis on an 8% SDS polyacrylamide slab gel, and transferred electrophoretically to a nitrocellulose filter (Schleicher and Schuell, Inc., Keene, NH) using established procedures (Ausubel *et al.* 1995). Following transfer, the filter was blocked by incubation with 2% bovine serum albumin (BSA) in TNT buffer (50 mm TRIS-HCl, pH 7.4, 100 mm NaCl, 0.1% Triton X-100) for 20 min at room temperature. After removal of the blocking solution, the filter was incubated for 1–2 hr at room temperature with TNT containing 2% BSA and either a 1:100

dilution (for Inp51p) or a 1:30 dilution (for Inp52p and Inp53p) of an affinity-purified preparation of the appropriate rabbit polyclonal antibody. To remove the excess primary antibody, the filter was washed sequentially, for 10 min each, with TN (50 mm TRIS-HCl, pH 7.4, 100 mm NaCl), with TNT, and again with TN, then incubated for 40 min at room temperature with an appropriate volume of TNT containing 2% BSA and a 1:5,000 dilution of donkey anti-rabbit IgG conjugated to horseradish peroxidase (Amersham, Arlington Heights, IL). The excess secondary antibody was removed by washing, as above, and the resulting immune-complexes were visualized using the ECL detection system (Amersham), according to the manufacturer. The rabbit polyclonal antibodies directed against Inp51p, Inp52p, and Inp53p were raised against appropriate C-terminal peptides using standard methods (Harlow and Lane 1988).

Metabolic labeling and analysis of inositol-containing compounds: Strains were inoculated at a density of 1×10^5 cells/ml in CM containing 20 μCi/ml of *myo*-[2-^{3}H(N)]inositol (American Radiolabeled Chemicals, St. Louis, MO), grown to a density of 1×10^7 cells/ml, collected by centrifugation, and washed with ice-cold H_2O. Cells were resuspended in 100 μl 0.5 N HCl, and, after the addition of 372 μl chloroform:methanol (1:2, v/v) and 100 μg acid-washed glass beads (Sigma Chemical Co., St. Louis), extracted by vigorous vortex mixing (bead beating) for 2 min. After addition of 125 μl each of chloroform and 2 M KCl, the mixture was subjected to vigorous vortex mixing for an additional 2 min. The resulting organic and aqueous phases were separated by centrifugation at 20,000 × *g* for 5 min. Inositol-containing lipids in the organic phase were resolved by thin layer chromatography on acid/oxalate-impregnated silica gel 60 thin layer plates as previously described (York and Majerus 1994). After spraying with En [^{3}H]ance (New England Nuclear, Boston), the plates were subjected to autoradiography and the relative amount of radioactivity in each species was quantitated by densitometric scanning.

Electron microscopy: Cells were fixed at 4° overnight with 2% glutaraldehyde in 150 mm Na-cacodylate (pH 7.2), washed with the same buffer lacking glutaraldehyde, postfixed on ice for 4 hr in the same buffer containing 2% osmium tetroxide, 1% potassium ferrocyanide, and 2.5 mm $CaCl_2$, washed again in the cacodylate buffer lacking fixative, and finally washed with 200 mm Na-acetate (pH 5.2). Samples of the resulting cells were stained with 1% uranyl acetate in the acetate buffer overnight, washed and dehydrated, sequentially, by incubation (for 30 min each) in 30%, 60%, 80% and 95% ethanol, and, finally, three times in absolute ethanol. The dehydrated cells were impregnated for 1.25 hr in Spurr resin:ethanol (1:1), for 5 hr in two changes of undiluted Spurr resin, and embedded in fresh resin, which was polymerized at 70° for 8 hr. Sections (90 nm) were cut on a microtome (Reichert-Jung, Vienna, Austria), stained with uranyl acetate, followed by Sato lead, washed, and examined in an electron microscope (Philips EM300; Philips Technologies, Cheshire, CT).

Staining with FM 4-64: Endocytic and vacuolar membranes were visualized by staining with the fluorescent vital dye FM 4-64 as described (Vida and Emr 1995). Briefly, cells were grown in YPD to midexponential phase, harvested by centrifugation, and resuspended in fresh YPD to a density of 1×10^9 cells/ml. FM 4-64 was added to a final concentration of 20 μm. The cells were then incubated either at 0° for 30 min or at 30° for 15 min, collected by brief centrifugation, and resuspended in fresh YPD at a density of 5×10^8 cells/ml. The cells were again incubated at either 4° or 30° for 45 min, recollected, placed on slides coated with gelatin, and viewed under an epifluorescence microscope (Carl Zeiss, Inc., Thornwood, NY) using a 546-nm cutoff filter.

RESULTS

A family of inositol polyphosphate 5-phosphatases in yeast: We initially identified a yeast gene highly related to mammalian 5-Ptases by comparing the deduced amino acid sequences of three mammalian 5-Ptases, 5-Ptase I (Z31695), 5-Ptase II (M74161), and OCRL-1 (M88162) (with the indicated GenBank accession numbers), to the predicted open reading frames in the then available *S. cerevisiae* genomic sequence. This gene, which we designated *INP51*, resides on chromosome IX, corresponds to locus YIL002c, and encodes a predicted product of 946 residues which we characterized in detail, as described elsewhere (L. E. Stolz, W. J. Kuo, J. Longchamps, M. K. Sekhon, and J. D. York, unpublished results). With the completion of the *S. cerevisiae* genome sequence, we found two additional open reading frames highly homologous to *INP51*. The *INP52* gene, locus YNL106c, lies on chromosome XIV and encodes a deduced product of 1183 residues. *INP53*, locus YOR109w, is situated on chromosome XV and encodes a predicted product of 1107 residues. If conservative amino acid substitutions are considered, Inp52p and Inp53p share ~70% similarity, whereas Inp51p is less related (~30% similarity) to the other two *INP5* gene products. Nonetheless, the presumptive C-terminal catalytic domains of all three gene products possess the signature motifs of demonstrated 5-Ptases (Figure 1). For example, identity to the consensus sequence, HDVIFWLGDLNYRI, is 71% for Inp51p and 85% for both Inp52p and Inp53p. Likewise, identity to a second highly conserved motif, PAWTDRILY is 100% for Inp51p and 77% for both Inp52p and Inp53p. In addition, the amino terminal halves of all three proteins share detectable similarity to the entire length of the 623-residue *S. cerevisiae SAC1* gene product (Figure 1). Although *SAC1* is not an essential gene, *sac1*Δ mutants are inositol auxotrophs and are cold-sensitive; moreover, particular *sac1* alleles suppress certain *act1*^{ts} alleles (Novick *et al.* 1989) and a *sac1*Δ mutation bypasses the effects of the *sec14-1*^{ts} mutation (Cleves *et al.* 1989; Whitters *et al.* 1993). The segment of Inp51p, Inp52p, and Inp53p with greatest similarity to Sac1p (100% identity for Inp52p and Inp53p; see Figure 1) corresponds to the portion of *SAC1* that is altered for suppression of *act1* and *sec14* mutations (Cleves *et al.* 1989). The amino terminal halves of Inp51p, Inp52p, and Inp53p are also similar to the 879-residue product of the YNL325c locus (Figure 1), which acts as a dosage suppressor of *sac1* mutations, although a *ynl325c* null mutation does not bypass *sec14* mutations (Kearns *et al.* 1997). The mammalian homolog of *INP51*, *INP52*, and *INP53* appears to be synaptojanin, which is a 5-Ptase associated with synaptic vesicles, that possesses a very similar domain structure (Figure 1). Finally, the C terminus of *INP52* contains a potential CAAX box or isoprenylation motif (CDPN-cooh) (Zhang and Casey 1996), like the mammalian 5-Ptase

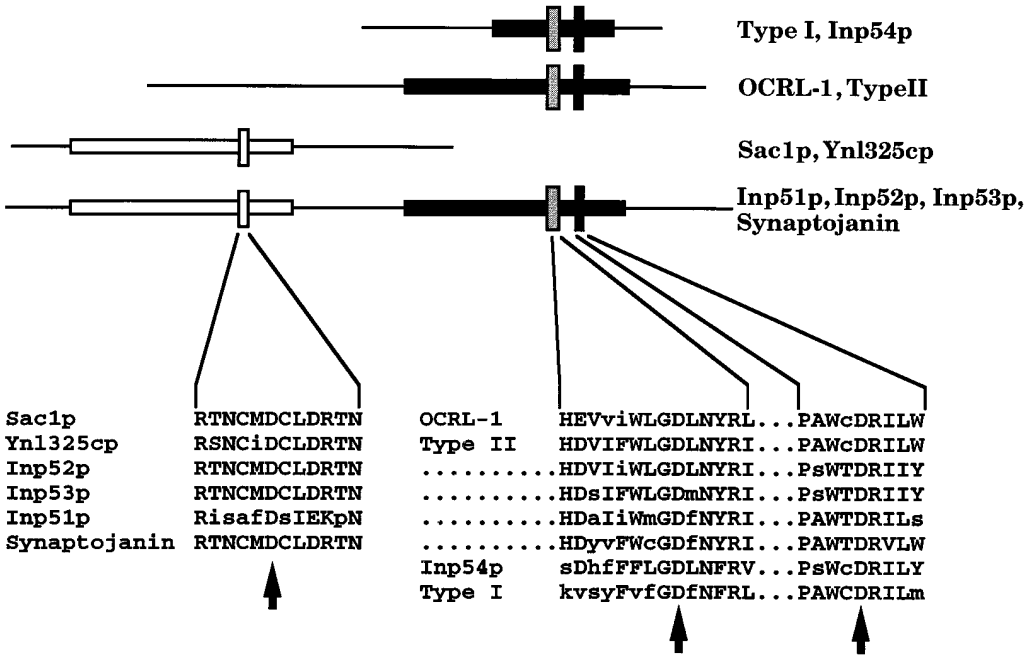

Figure 1.—Schematic representation of the domain structure of Inp51p, Inp52p, Inp53p, and Inp54p. The catalytic domains of known 5-Ptases (5-Ptase I, OCRL-1, 5-Ptase II, and synaptojanin) are shown as solid bars. The relative positions, consensus sequences, and alignment with Inp51p, Inp52p, Inp53p, and Inp54p of two sequence motifs diagnostic of 5-Ptases are indicated. The arrows in this domain indicate residues that are critical for catalytic activity. The Sac1p-like domain present in synpatojanin and in Inp51p, Inp52p, and Inp53p is shown as the open bar. The position, consensus sequence, and alignment to Inp51p, Inp52p, and Inp53p, of a characteristic feature of the Sac1p-like domain is also indicated. The arrow in this domain indicates the conserved D residue (corresponding to the D^{422} in Sac1p; see Kearns *et al.* 1997) that is necessary for the suppression activities of Sac1p.

I and 5-Ptase II (De Smedt *et al.* 1996; Jefferson and Majerus 1995).

Additionally, we have identified a fourth putative 5-Ptase open reading frame in the *S. cerevisiae* genome which contains the two catalytic motifs described above. This open reading frame, which we designate *INP54*, corresponds to locus YOL065c on chromosome XV and encodes a predicted product of 384 residues. Significantly, Inp54p differs from the other three yeast 5-Ptases in that it lacks the Sac1p-like domain and based on its smaller size most resembles the mammalian Type I 5-Ptase (Figure 1).

Genetic analysis of *INP51*, *INP52*, and *INP53* function: To ascertain the roles that the *INP51*, *INP52*, and *INP53* gene products play in the physiology of the yeast cell, we constructed mutant strains deficient in one or more of these proteins and examined their phenotype. A null mutation, *inp51::LEU2*, was constructed previously (L. E. Stolz, W. J. Kuo, J. Longchamps, M. K. Sekhon, and J. D. York, unpublished results). As described in materials and methods, we also generated null mutations, *inp52::HIS3* and *inp53::HIS3*, in the other two loci. Upon sporulation and tetrad dissection of each heterozygous diploid, four-spored tetrads were readily recovered in which the marker (either Leu^+ or His^+) segregated 2:2. Hence, *inp51*, *inp52*, and *inp53* single mutants are all viable. The *inp51::LEU2* and *inp52::HIS3* spore clones appeared normal. In contrast, *inp53::HIS3* spores yielded very small colonies compared to their sister His^- (*INP53*$^+$) spores. Upon restreaking, however, the *inp53::HIS3* cells grew at a rate comparable to the wild-type cells (data not shown), suggesting that loss of Inp53p may cause a defect in germination.

To verify that *INP51*, *INP52*, and *INP53* are expressed and to confirm that the null mutations prevented production of the corresponding polypeptides, we raised specific rabbit polyclonal antibodies directed against the Inp51p, Inp52p, and Inp53p proteins. Extracts of a wild-type haploid derived from the parental strain and of each single mutant were prepared and separated into soluble and particulate fractions. The proteins present were resolved by SDS-PAGE and examined by immunoblotting. In wild-type cells, each of the three proteins was found primarily in the particulate fraction and displayed an apparent molecular mass—Inp51p (108 kD), Inp52p (133–136 kD), and Inp53p (124–125 kD)—consistent with the molecular weight calculated from its deduced amino acid sequence (Figure 2). Since the extracts examined were prepared by lysis of thoroughly washed spheroplasts (see materials and methods), this distribution suggests that all three proteins are membrane-associated. As expected, the *inp51* mutant lacked the 108 kD species but retained the 133 and 125 kD species; likewise, the *inp52* mutant only lacked the

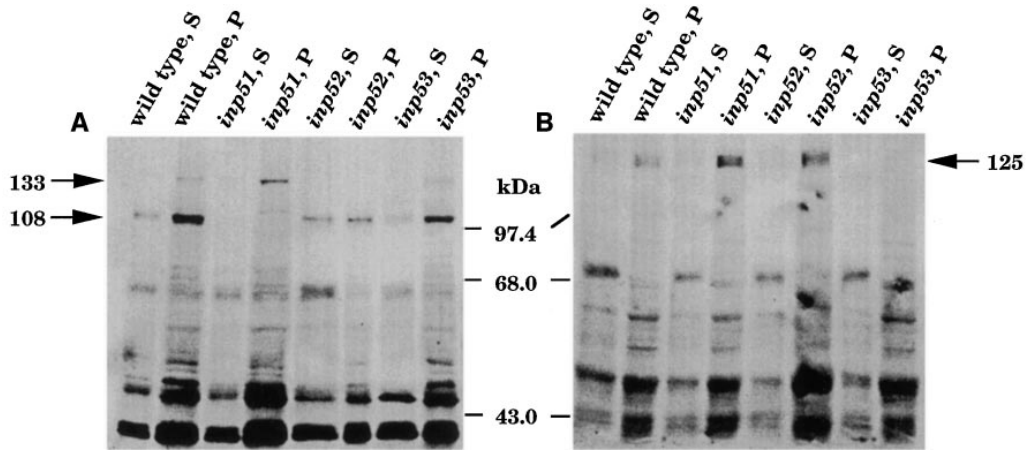

Figure 2.—Immunoblot analysis of Inp51p, Inp52p, and Inp53p expression. (A) Samples of spheroplast lysates of the parental strain (wild type) and the indicated *inp51*, *inp52*, or *inp53* null mutants were fractionated by differential centrifugation into a pellet (P) and a soluble (S) fraction. Portions of these fractions were resolved by SDS-PAGE, transferred to a nitrocellulose filter, and probed simultaneously with both anti-Inp51p and anti-Inp52p antibodies. (B) As in A, except that the blots were probed with anti-Inp53p antibodies. Positions of molecular weight markers are given. Relative migration (arrowheads) and apparent molecular masses are indicated for Inp51p (108 kD), Inp52p (133 kD), and Inp53p (125 kD).

133 kD protein (Figure 2A), and the *inp53* mutant was only missing the 125 kD band (Figure 2B).

Since all three genes are expressed, the lack of overt phenotype of the three single mutants, and their homology to each other, suggested that the genes might be functionally redundant. To test this possibility, we used pairwise crosses and tetrad dissection (see materials and methods) to isolate all three double mutant combinations. Like the single mutants, we found that *inp51 inp52*, *inp51 inp53*, and *inp52 inp53* double mutant spores were obtained at the expected frequency, indicating that cells lacking two of the three gene products are still viable. However, the *inp51 inp52* and the *inp52 inp53* double mutant spores both grew distinctly slower than wild-type spore clones; the *inp51 inp52* clones exhibited a greater degree of growth inhibition. These growth properties were reproducibly observed upon restreaking the double mutants onto growth media at 30° (Figure 3), and thus do not reflect effects on spore germination. In contrast, the *inp51 inp53* double mutant germinated and grew at rates indistinguishable from wild-type cells (Figure 3).

We have noted previously that our parental strain (W303) grows poorly at temperatures below 15°, while the *inp51* null mutation confers the ability to grow vigorously at such low temperatures ("cold tolerance") (L. E. Stolz, W. J. Kuo, J. Longchamps, M. K. Sekhon, and J. D. York, unpublished results). Therefore, we examined both the *inp52* and *inp53* single mutants, and the three double mutants, for their ability to grow at a variety of temperatures (12°, 18°, 23°, 30° and 37°) on rich medium. There were no growth differences between the single mutant cells and the wild type cells at 18°, 23°, 30° and 37° (data not shown). Unlike the *inp51* mutation, neither the *inp52* nor the *inp53* mutation exhibited a dramatic improvement in growth at 12° (although the *inp52* mutation had some modest effect) (Figure 3A). The *inp51 inp53* and the *inp52 inp53* double mutants showed at least as vigorous growth at 12° as the *inp51* single mutant, whereas the *inp51 inp52* cells grew no better than the *inp52* single mutant (Figure 3A). To confirm that these growth effects were not simply due to differences in the number of viable cells applied to the plates, we dispersed individual cells using a micromanipulator and followed their growth under the microscope. At least five different cells were followed for each strain tested at 12° and 30°. We consistently observed, in agreement with the streak tests, that *inp51* single mutants and *inp51 inp53* and *inp52 inp53* double mutants are able to grow at 12° (Figure 3B and Table 2). In addition, the *inp52* single mutants and the *inp51 inp52* double mutants demonstrate some mild cold tolerance, whereas the parental strain and the *inp53* single mutants do not grow at 12°. Collectively, the growth phenotypes of the single mutants, and the genetic interactions observed in the double mutants, suggest that Inp51p, Inp52p, and Inp53p have some distinct roles in the cell, despite their sequence relatedness and presumed catalytic function.

Loss of Inp51p detectably increases the cellular pool of PtdIns[4,5]P_2: If Inp51p, Inp52p, and Inp53p serve as 5-Ptases *in vivo*, then the loss of these enzymes might lead to detectable perturbations in the cellular levels of PtdIns[4,5]P_2 or Ins[1,4,5]P_3 (or both). Such changes could provide some insight into the phenotypes of the mutants. Indeed, we report elsewhere that *inp51* mutants do exhibit an increase in both the PtdIns[4,5]P_2 and Ins[1,4,5]P_3 pools as compared to wild-type cells (L. E. Stolz, W. J. Kuo, J. Longchamps, M. K. Sekhon, and J. D. York, unpublished results). It was of obvious interest to determine if the loss of Inp52p and Inp53p, alone or in combination with each other or Inp51p,

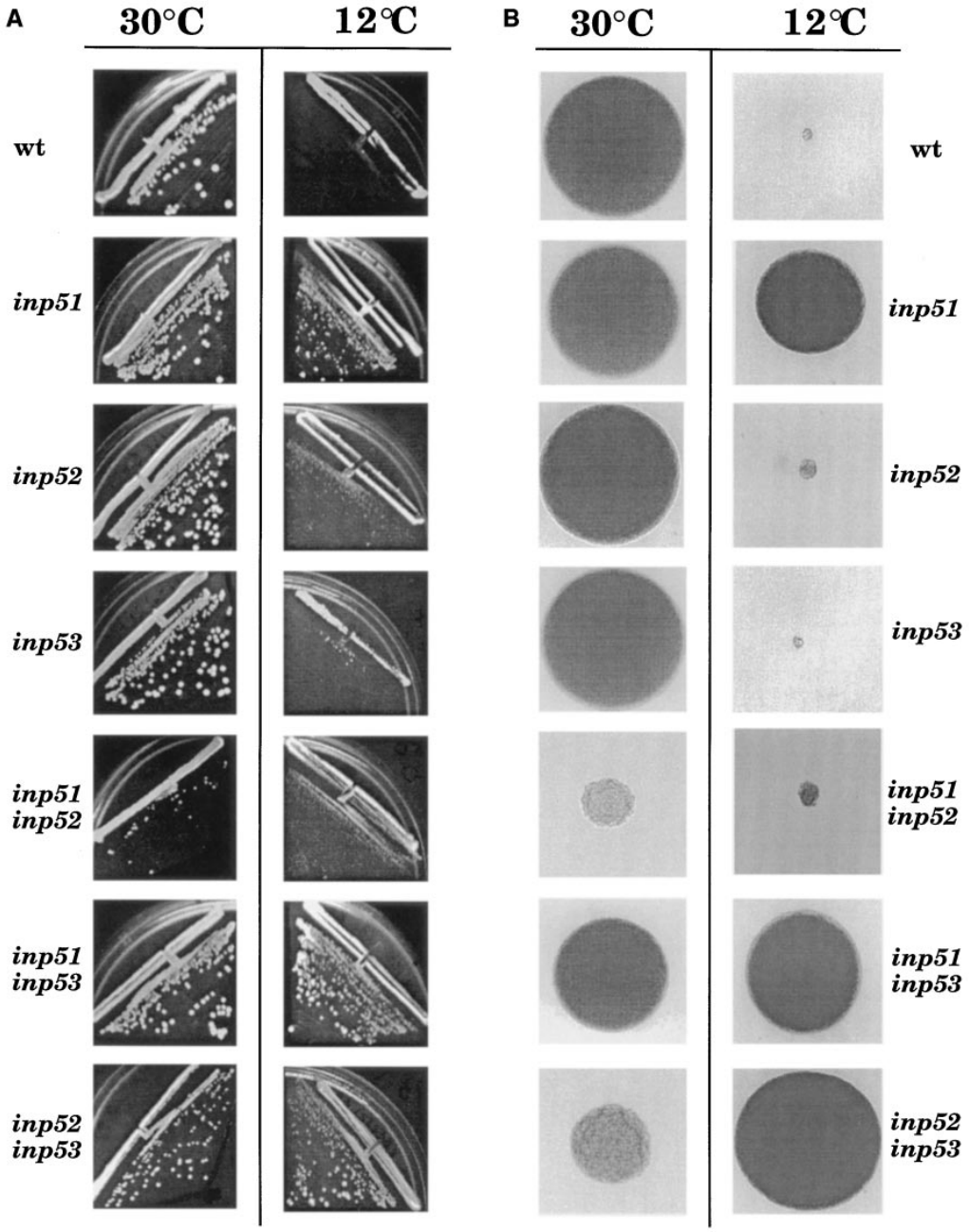

Figure 3.—Analysis of the cold-tolerant phenotype. (A) The indicated strains were streaked on YPD plates and incubated for 2 days (at 30°) or for two weeks (at 12°). Each picture is representative of a large number of independent streaks. (B) Individual cells were distributed with a micromanipulator and incubated at either 30° for two days or at 12° for two weeks, and then observed under the 40× objective of a dissection microscope (Carl Zeiss, Inc.) and photographed. Each picture is representative of five individual colonies viewed.

might also have some effect. Cultures of the parental strain, the three single mutants, and the three double mutants were labeled with [^{3}H]inositol to a steady-state. The incorporation of ^{3}H into PtdInsP$_2$ was analyzed by an oxalate-TLC method capable of resolving PtdIns, PtdInsP and PtdInsP$_2$, as described in materials and methods. In each of the strains carrying the *inp51* null mutation (Table 3), the level of PtdInsP$_2$ (presumably PtdIns[4,5]P$_2$) was elevated two- to threefold as compared to the control cells, whereas the loss of either *inp52* or *inp53*, or both, had no detectable effect. Moreover, neither the *inp52* mutation nor the *inp53* mutation, when combined with the *inp51* mutation, caused any further increase in the accumulation of PtdInsP$_2$ (above the *inp51* single mutation). Likewise, examination of the inositol phosphates in the soluble fraction by HPLC, showed an increase in the levels of Ins[1,4,5]P$_3$ in the *inp51* cells as compared to the wild-type control; however, the *inp52* and *inp53* single mutants showed no detectable increase (data not shown). These results suggest that Inp51p is the major 5-Ptase in *S. cerevisiae* and/or that the bulk of the cellular pool of PtdIns-[4,5]P$_2$ is accessible to Inp51p, but not to Inp52p or Inp53p. It is noteworthy that during revision of this manuscript Dove *et al.* (1997) reported the identification of PtdIns[3,5]P$_2$ in *S. cerevisiae* which is transiently formed in response to hyperosmotic stress. Thus, an alternative possibility is that Inp52p and/or Inp53p utilize PtdIns[3,5]P$_2$ and not PtdIns[4,5]P$_2$. Since our labeling studies were performed in the absence of hyper-

TABLE 2

Growth of yeast colonies at 12°

Strain	Average colony diameter (μm)[a]	Fold increase (two-tailed *t*-test *P* value)
W303	24 ± 0.182	1
inp51::LEU2	366 ± 3.318	15.3 (< 0.001)
inp52::HIS3	65 ± 0.158	2.7 (< 0.001)
inp53::HIS3	31 ± 0.311	1.3 (n/a)
inp51::LEU2 inp52::HIS3	83 ± 0.914	3.4 (< 0.001)
inp51::LEU2 inp53::HIS3	434 ± 4.341	18.1 (< 0.001)
inp52::HIS3 inp53::HIS3	514 ± 3.737	21.4 (< 0.001)

[a] Represents the average and standard deviation from a minimum of 5 colonies. *P* value derived from two-tailed student's *t*-test.

osmotic stress, accumulation of this species in the appropriate *inp5* null strains may have been missed.

Evidence that *INP51, INP52,* and *INP53* have an overlapping function: Certain physiological functions in *S. cerevisiae* are carried out by related genes comprising an essential gene set. For example, there are three genes (*TPK1*, *TPK2*, and *TPK3*) that encode the catalytic subunit of cAMP-dependent protein kinase, and there are three genes that encode the G1 cyclins (*CLN1*, *CLN2*, and *CLN3*). To definitively establish whether *INP51*, *INP52*, and *INP53* might constitute an essential gene set, we carried out appropriate genetic crosses (see materials and methods) to generate a diploid strain heterozygous for all three null mutations. After sporulation and dissection, many of the tetrads segregated 3:1 for live:dead spores (Figure 4A) while the deduced triple mutant spores were always inviable (Figure 4A). To confirm that this segregation pattern was due exclusively to loss of the three gene products, the same heterozygous diploid was transformed with a *URA3*-marked *CEN* plasmid (pRS316) carrying the *INP51* gene driven by its own promoter. As expected, upon sporulation and dissection of the plasmid-containing diploid, the majority of tetrads now segregated 4:0 for live:dead (Figure 4B). The deduced triple (Leu^+ His^+) mutant spores were viable (Figure 4C), and always Ura^+. The plasmid-containing triple mutant strain was unable to grow on plates containing 5-FOA (Figure 4D), whereas control cells grew well on this medium (Figure 4E).

Examination of the presumptive *inp51 inp52 inp53* spore clones under the microscope revealed that the cells proceed through four or five divisions before growth ceases when germinated on YPD medium (Figure 4F). However, when triple mutant spores were germinated on YPD plates supplemented with 1 M sorbitol and incubated at 23°, the cells were able to propagate continuously (Figure 4G), although at a rate much slower than that of wild-type cells.

TABLE 3

Measurement of PtdIns(4,5)P_2 levels *in vivo*

Strain	PtdIns(4,5)P_2[a]
W303	52.2
inp51::LEU2	105.2 (P = 0.02)
inp52::HIS3	45.6
inp53::HIS3	47.8
inp51::LEU2 inp52::HIS3	103.8 (P = 0.02)
inp51::LEU2 inp53::HIS3	110.5 (P = 0.02)
inp52::HIS3 inp53::HIS3	44.4

[a] Levels of lipid from 3 experiments are expressed as arbitrary densitometry units normalized with respect to 20,000 PtdIns units. Less than 10% standard deviation was observed. *P* value derived from two-tailed student's *t*-test.

Morphological effects of the loss of *INP51, INP52,* and *INP53*: Because both lipid-linked and soluble inositol phosphates have been implicated in membrane trafficking and other processes that might affect cell morphology, we used electron microscopy to examine the effects of *inp51*, *inp52*, and *inp53* mutations at the ultrastructural level. Cells were grown to midexponential phase at 30° and prepared for electron microscopy, as described in materials and methods. Compared to the parental strain (W303), which had a large central vacuole and a smooth interface between the plasma membrane and the relatively thin (~200 nm) cell wall (Figure 5A), the *inp51* and *inp52* single mutants displayed no obvious differences (data not shown). In marked contrast, the *inp53* single mutant and all three of the double mutants manifested, to different degrees, readily observable abnormalities, especially in the plasma membrane and the cell wall. In the *inp53* mutant, and the *inp51 inp53* double mutant, the wall (most prominently in the mother cell) is noticeably thicker (~300 nm), the plasma membrane appears to have increased in-pocketing, and the vacuole seems irregularly shaped (Figure 5, B and D). Gross morphological defects were found in the *inp51 inp52* double mutant, wherein the plasma membrane displays enormous invaginations and convolutions, with corresponding abnor-

mal depositions of cell wall material, and vesiculation of other cellular membranes (Figure 5C). These effects appear to be largely confined to mother cells, suggesting that this phenotype is the result of cumulative or age-related damage. In support of this hypothesis, we observed that, in exponentially growing cultures, only about 20% of the population displayed striking morphological defects, whereas 70% were mildly deformed, and 10% appeared relatively normal. Equally dramatic, the *inp52 inp53* double mutant displayed clearly fragmented internal membranes and a pronounced thickening of the cell wall (≥500 nm), which was detectable in both the mother and daughter cells (Figure 5E). Finally, we examined the *inp51 inp52 inp53* triple mutant, which was propagated on medium containing 1 M sorbitol. These cells (both mother and bud) were clearly misshapen, containing markedly thickened (and even double-layered) cell walls, grossly distorted plasma membranes, and fragmentation of internal membranes (Figure 5F). The phenotype of the triple mutant suggests that loss of all three enzymes greatly exacerbates the effects of the absence of any individual enzyme.

Recently, Luo and Chang (1997), using a mutant form of the plasma membrane H^+-ATPase (Pma1p) that is shunted to the vacuole instead of its normal destination, selected suppressor mutations that allow for normal trafficking of Pma1p. Presumably, suppressors perturb the normal cellular mechanisms that ensure that defective plasma membrane proteins are endocytosed and diverted to the vacuole for destruction. Indeed, among the mutations isolated in this selection were various *VPS* loci that prevent normal vacuolar biogenesis, other loci that interfere with endosome-to-vacuole traffic, and a third class that appears to perturb endosome-to-Golgi recycling. One of the genes in this third class was *SOP2*, which is identical to the *INP53* gene we describe here. As a result, we wanted to determine whether loss of Inp51p, Inp52p, and Inp53p, causes abnormalities in endocytosis. Therefore, we stained cells with the fluorophor FM 4-64, which binds specifically to the membranes of endocytic vesicles and vacuoles (Vida and Emr 1995). We found that compared to the parental cells (Figure 6, A and B), the *inp51*, *inp52*, and *inp53* (Figure 6, C and D) single mutants, and *inp51 inp53* and *inp52 inp53* double mutants (data not shown), had no obvious defect in endocytosis. However, in agreement with the observations made from the electron microscope, the *inp51 inp52* double mutants exhibited small, highly fragmented vacuoles, indicating a de-

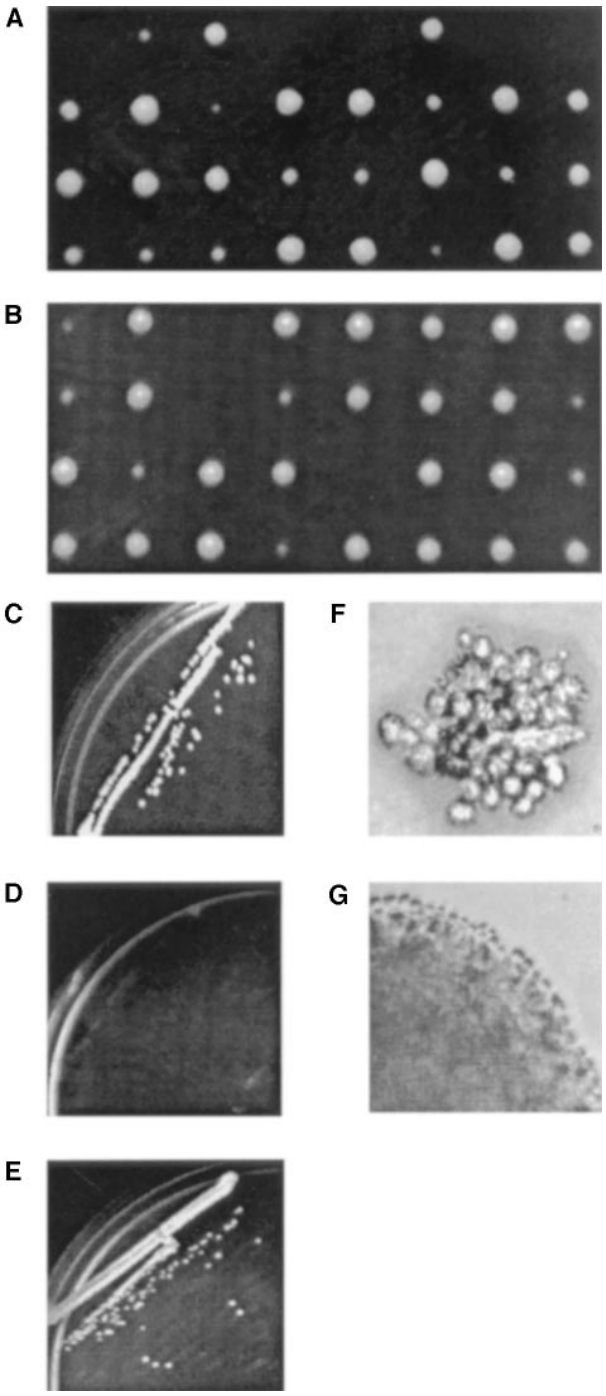

Figure 4—Segregation analysis of the *inp51 inp52 inp53* triple mutant. (A) Tetrads from dissection of an *inp51::LEU2*/*INP51 inp52::HIS3*/*INP52 inp53::HIS3*/*INP53* heterozygous diploid. Note that live:dead segregated 3:1 in the majority (5-out-of-8) of the asci shown. (B) Tetrads from dissection of an *inp51::LEU2*/*INP51 inp52::HIS3*/*INP52 inp53::HIS3*/*INP53* heterozygous diploid carrying the *INP51* gene expressed from its own promoter on the *URA3*-marked *CEN* vector, pRS316. Note that live:dead segregates 4:0 in the majority (6-out-of-8) of the asci shown. The *inp51 inp52 inp53* triple mutant containing the complementing *INP51* plasmid is able to grow when streaked on YPD plates (C), but unable to grow on medium containing 5-FOA (D), whereas the parental cells grow normally on 5-FOA-containing medium (E). Growth of the deduced *inp51 inp52 inp53* spore clones on YPD plates (F) and on the same medium supplemented with 1 M sorbitol (G), was photographed as described in the legend to Figure 3B.

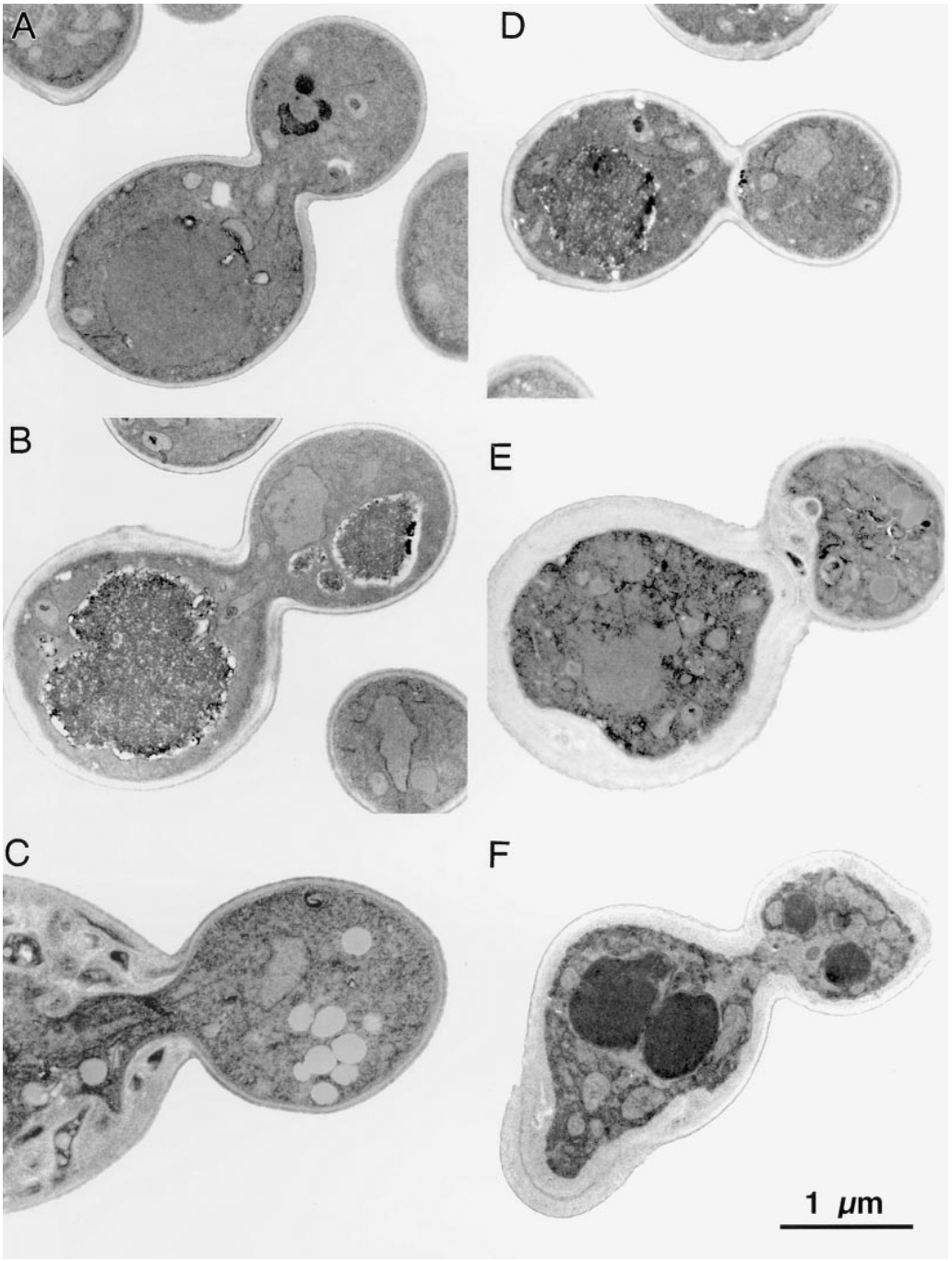

Figure 5.—Analysis of the effects of *inp51*, *inp52*, and *inp53* mutations on cell morphology. Cultures of the mutants shown were grown to midexponential phase and prepared for electron microscopy, as described in materials and methods. Micrographs are representative of numerous cells of each strain examined. (A) Wild-type (*INP51*$^+$ *INP52*$^+$ *INP53*$^+$) cells; (B) an *inp53* single mutant; (C) an *inp51 inp52* double mutant; (D) an *inp51 inp53* double mutant; (E) an *inp52 inp53* double mutant; and (F) the *inp51 inp52 inp53* triple mutant propagated in medium containing 1 M sorbitol.

fect in vacuole formation and/or in maintenance of vacuolar integrity (Figure 6, E and F).

DISCUSSION

Mammalian cells possess at least ten distinct 5-Ptase isoforms (reviewed in Drayer *et al.* 1996; Irvine 1992; Majerus 1996; Mitchell *et al.* 1996). Some of this complexity can be attributed to tissue- and/or development-specific enzyme functions. However, since at least four different representatives of 5-Ptases are present in budding yeast, a unicellular eukaryote, these enzymes must have distinct and conserved functions in eukaryotic cell physiology. Indeed, our genetic analysis of the *S. cerevisiae INP51*, *INP52*, and *INP53* genes supports the view that the corresponding enzymes are not simply redundant isozymes. First, although *inp51*, *inp52*, and *inp53* single mutants are all viable, only the *inp53* mutation appeared to affect germination. Second, whereas an *inp51* mutation conferred cold tolerance in our strain background, *inp52* and *inp53* mutations did not. Third, although the primary structures of Inp52p and Inp53p are more closely related to each other than either protein is to Inp51p, loss of Inp52p and Inp53p did not

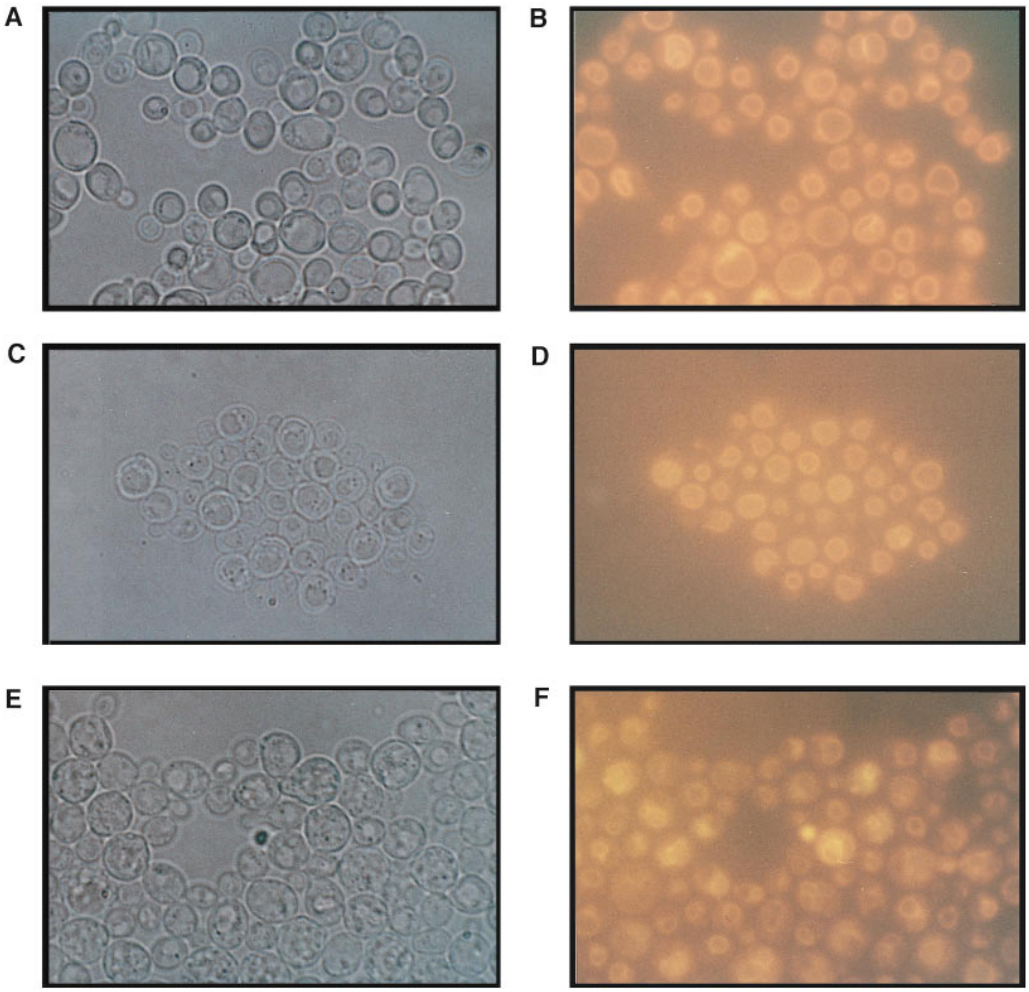

Figure 6.—Analysis of vacuolar and endocytic membranes with a fluorescent dye. Images show bright field (left column) and fluorescent (right column) views of the following strains, which we stained with the vital dye, FM 4-64, and observed as described in materials and methods. Wild-type cells (A and B); *inp53* single mutants (C and D); and *inp51 inp52* double mutants (E and F).

yield equivalent phenotypes when combined with an *inp51* mutation. For example, an *inp51 inp52* double mutant displayed much more severe morphological defects than did an *inp51 inp53* double mutant. Conversely, some of our observations support the conclusion that Inp52p and Inp53p do share some functional relatedness, since an *inp52* mutation significantly potentiated the mild morphological defect of an *inp53* mutant, but an *inp51* mutation did not. Finally, since *INP54* is unable to compensate for the lethality of the *inp51 inp52 inp53* triple mutant and, since it lacks the Sac1-like domain, it appears to be functionally distinct. The phenotypes of our mutant strains are summarized in Table 4.

One possible model to explain these differential effects is that Inp51p acts in pathways or processes largely (but not completely) distinct from those involving Inp52p, and that Inp53p has a minor role (in terms of amount or activity) in both pathways, at least in vegetatively-growing cells. Inp54p has a completely distinct function in the cell. By this model, an *inp51* single mutant survives because it can still carry out Inp52p-dependent events and, through Inp53p, can bypass the need for Inp51p. Likewise, an *inp52* single mutant survives because it can carry out Inp51p-dependent events, and through Inp53p, can bypass the need for Inp52p. An *inp53* single mutant survives because it can carry out both Inp51p- and Inp52p-dependent events. The fact that *inp53* single mutants showed a mild germination defect and a mild morphological defect, especially in older mother cells, suggests that Inp53p may normally function primarily at stationary phase and/or under conditions of nutritional stress. Again, according to the proposed model, since the *INP51* and *INP52* gene products are postulated to have roles in two, largely separable, cellular pathways, combining null mutations in these two genes would be expected to yield the most severe phenotype, as was observed. In contrast, removal of *INP53*, since it is presumed to play a minor role in the *INP51*-dependent pathway would not be expected to markedly exacerbate the phenotype of an *inp51* mutation; however, since Inp53p has some functional redundancy with Inp52p, removal of both *INP52* and *INP53* would completely block the *INP52*-dependent pathway, leading to a readily detectable growth phenotype, as we also found.

The fact that yeast can survive without all three enzymes, as long as osmotic support (1 M sorbitol) was provided in the medium, suggests that the major effect

TABLE 4

Summary of phenotypes of mutant yeast strains

Strain	Phenotype[a]			
	Growth	Cold tolerance	PtdIns(4,5)P_2 levels	Morphology
W303 (wt)	++++	−	1.0	Thin cell wall, smooth PM, large, round vacuole
inp51	++++	+++	2.0	Wild-type-like
inp52	++++	+	0.87	Wild-type-like
inp53	++++, germination defect	−	0.92	Slightly thickened cell wall, PM invaginations, irregularly shaped vacuole
inp51 inp52	++	+	2.0	Abnormal cell wall depositions, highly disrupted PM, small, fragmented vacuole
inp51 inp53	++++	+++	2.1	Slightly thickened cell wall, PM invaginations, irregularly shaped vacuole
inp52 inp53	+++	+++	0.85	Very thick cell wall, PM invaginations and distortions, fragmented internal structures
inp51 inp52 inp53	−	ND	ND	Inviable
inp51 inp52 inp53, grown in presence of 1 M Sorbitol	+	ND	ND	Thick/double layer of cell wall, PM invaginations and distortions, fragmented internal structures, misshapen cells

[a] In the growth and cold tolerance columns, + indicates growth, − indicates no growth, and ND, not determined. Levels of PtdIns(4,5)P_2 are standardized to wild-type levels (see Table 3 for further information).

of the absence of these enzymes is a defect in membrane and/or cell wall structure and function, as was clearly confirmed by our ultrastructural analysis. However, sorbitol has been reported to have rather pleiotropic effects. In at least one strain background, 1 M sorbitol can rescue the lethality of a null mutation (*stt4*Δ) in a demonstrated PtdIns 4-kinase (Yoshida *et al.* 1994). Other studies suggest that sorbitol can alter actin cytoskeleton organization (Chowdhury *et al.* 1992), induce expression of some heat shock genes (Varela *et al.* 1992), increase the cytosolic glycerol concentration (Reed *et al.* 1987), and ameliorate the deleterious effects of the loss of certain phosphoprotein phosphatases and protein kinases (McLaughlin *et al.* 1996; Posas *et al.* 1993), including *PKC1* (Levin and Bartlett-Heubusch 1992), which participates in a signal transduction pathway necessary for the maintenance of cell wall integrity.

Inp51p, Inp52p, and Inp53p are all expressed in exponentially-growing cells and seem to be associated largely with the particulate fraction, suggesting that each is membrane-associated. However, only *inp51* mutations caused a detectable elevation in the total cellular pool of PtdIns[4,5]P_2 and showed no further elevation when combined with either *inp52* or *inp53* mutations, suggesting that Inp51p is either responsible for the bulk of the PtdIns[4,5]P_2-specific 5-Ptase activity in the cell or, alternatively, that it is localized to the cellular membranes that contain the highest PtdIns[4,5]P_2 content. In this regard, it would be useful to determine the subcellular localization of these three enzymes. However, despite affinity-purification of the polyclonal antibodies, the expression level of each protein is too low to allow reliable detection by indirect immunofluorescence. Other approaches are in progress to address this important question, as well as related issues, such as the role, if any, of the potential CAAX box at the C terminus of Inp52p in its subcellular targeting. Another possibility to explain the inositol labeling results is that Inp51p is specific for PtdIns[4,5]P_2 as a substrate, while Inp52p and Inp53p might act only on soluble inositol 5-phosphates. However, loss of Inp52p or Inp53p, or both, did not detectably elevate the cellular content of Ins[1,4,5]P_3.

We have demonstrated elsewhere that the cold-tolerant phenotype of *inp51* null strain correlates with the accumulation of PtdIns[4,5]P_2 and does not require the production of soluble inositol phosphates (L. E. Stolz, W. J. Kuo, J. Longchamps, M. K. Sekhon, and J. D. York, unpublished results). Consistent with this observation, *inp52* or *inp53* null strains do not show measurable increases of PtdIns[4,5]P_2 and do not exhibit cold-

tolerant growth. Furthermore, the *inp51 inp52* and the *inp51 inp53* double mutants do not exhibit additive increases in either PtdIns[4,5]P_2 or in growth rates at cold temperatures. A notable exception is the *inp52 inp53* double mutant which is cold-tolerant despite the fact that increases in PtdIns[4,5]P_2 were not detected. This leaves open the possibilities that either some other metabolite or changes in a minor pool of PtdIns[4,5]P_2 (which are undetectable by our method) are sufficient for enabling the cold-tolerant growth. The mechanism by which cold resistance occurs is uncertain. We were unable to find reports of yeast deletion mutations that resulted in cold-tolerance; however, many mutations have been shown to result in cold-sensitivity. Mutations in the tryptophan biosynthetic pathway result in cold-sensitivity, presumably because the tryptophan permease cannot function at cold temperatures (Singh and Manney 1974). Since our background W303 strain carries a *trp1-1* allele, its cold-sensitivity may likely be due to a defect in this permease. We suggest that loss of certain 5-ptase activities may result in restoring tryptophan permease function at cold temperatures.

Inp51p, Inp52p, and Inp53p are most closely related to mammalian synaptojanin both because of sequence relatedness and because synaptojanin and the three yeast proteins all contain an N-terminal domain homologous to Sac1p, which, in *S. cerevisiae*, is an integral membrane protein associated primarily with the Golgi compartment. Synaptojanin is colocalized to synaptic vesicles in presynaptic nerve terminals with the coated pit-associated GTPase, dynamin, and interacts with the SH2- and SH3-domains of Grb2 (McPherson *et al.* 1994a,b). It has been proposed that synaptojanin links phosphoinositide metabolism with synaptic vesicle recycling, an endocytic process (McPherson *et al.* 1996; Stack *et al.* 1995), because PtdIns[4,5]P_2 plays a role in stimulus-coupled secretion (Hay *et al.* 1995), synaptojanin can utilize PtdIns[4,5]P_2 as a substrate, and synaptojanin contains a Sac1p-related domain. Our results, and those of Luo and Chang (1997), suggest that, like neuronal synaptojanin, Inp51p, Inp52p, and Inp53p may play roles in vesicle trafficking. However, *inp51*, *inp52*, and *inp53* mutants do not exhibit any defects in carboxypeptidase Y sorting, a marker for vacuolar sorting defects (Srinivasan *et al.* 1997).

The function of the Sac1p-like domain in synaptojanin and in Inp51p, Inp52p, and Inp53p is unclear. Null mutations in the *SAC1* gene suppress Golgi transport defects and the inviability of a *sec14*^{ts} mutation at the restrictive temperature (Cleves *et al.* 1989; Whitters *et al.* 1993). Sec14p is a phospholipid transfer protein specific for PtdIns and phosphatidylcholine. Likewise, loss of function *sac1* alleles suppress the secretory transport defects manifested by certain actin (*act1*^{ts}) alleles and exacerbate the effects of others (Cleves *et al.* 1989; Novick *et al.* 1989). It has also been reported that Sac1p is a transport protein responsible for the entry of ATP into the lumen of the endoplasmic reticulum, where the nucleotide is needed for the translocation of nascent secretory proteins (Mayinger *et al.* 1995). However, more recent evidence indicates that defects in Sac1p bypass the requirement for Sec14p by causing an increase in the pool of diacylglycerol in Golgi membranes (Kearns *et al.* 1997). Nevertheless, unlike a *sac1*Δ mutation, *inp51*Δ, *inp52*Δ, and *inp53*Δ mutations fail to "bypass" the Sec14p requirement, suggesting that despite the sequence similarity of the N-terminal domains of Inp51p, Inp52p, and Inp53p to Sac1p, these regions in the 5-Ptases may have a different function. We report elsewhere that deletion of the Sac1p-like domain (residues 2 to 490) of Inp51p results in a twofold increase in the level of PtdIns[4,5]P_2 *in vivo*, consistent with the notion that this domain is required for proper cellular 5-Ptase function accumulation (L. E. Stolz, W. J. Kuo, J. Longchamps, M. K. Sekhon, and J. D. York, unpublished results). However, it is unclear whether the loss of function of the Sac1-less Inp51p is due to a loss of intrinsic activity or improper localization. In addition, a D^{426}→A point mutation in the Sac1p-like domain of Inp51p does not result in lipid accumulation (L. E. Stolz, W. J. Kuo, J. Longchamps, M. K. Sekhon, and J. D. York, unpublished results). This is of interest because the mutations of the cognate D residue in Sac1p to N (indicated by the arrow in Figure 1) as found in the *sac1-8* and *sac1-22* alleles are able to create a "bypass" phenotype (Kearns *et al.* 1997). Thus, this residue in 5-Ptase does not appear to be required for function. Experiments to further explore the role of the Sac1p-like domains in Inp51p, Inp52p, and Inp53p are in progress.

There is considerable evidence that PtdIns[4,5]P_2 modulates the activity of certain actin-binding proteins, such as profilin. It was conceivable, therefore, that loss of *INP51*, *INP52*, and/or *INP53* might cause defects in the actin cytoskeleton. However, staining of *inp51*, *inp52*, and *inp53* mutants, and all three double mutants, with rhodamine-phalloidin did not reveal any obvious abnormality in the distribution of filamentous actin in these cells (unpublished observations). In this same regard, another enzyme responsible for the removal of PtdIns[4,5]P_2 is the Plc1p phospholipase (Flick and Thorner 1993). However, an *inp51 plc1* double mutant (and an *inp51 inp53 plc1* triple mutant), in which it might be anticipated that the cellular PtdIns[4,5]P_2 pool has a further elevation over that caused by an *inp51* mutation alone (although this supposition was not examined by direct chemical analysis) did not show any obvious enhancement of the growth phenotypes associated with either the *inp51* single mutation or the *inp51 inp53* double mutation (unpublished observations). In contrast to the loss of these degradative enzymes, inactivation of the genes for either of the demonstrated PtdIns 4-kinases, *PIK1* (Flanagan *et al.* 1993) and *STT4* (Yoshida *et al.* 1994), necessary for the synthesis of

PtdIns[4,5]P_2 in *S. cerevisiae*, is lethal. Likewise, the genes for other presumed lipid kinases in yeast, such as *TOR2* (Kunz *et al.* 1993), are essential for viability.

During preparation of this manuscript, it came to our attention that an independent study (Srinivasan *et al.* 1997) has also concluded that the *INP51*, *INP52*, and *INP53* genes (which were designated *SJL1*, *SJL2*, and *SJL3*) constitute an essential gene family and that mutations in these genes display phenotypes with respect to both growth and morphology in substantial agreement with the results we have presented here.

Finally, during revision of this manuscript the existence of PtdIns[3,5]P_2 in yeast was reported (Dove *et al.* 1997). Under conditions of hyperosmotic stress as induced by high concentrations of sorbitol or sodium chloride, yeast transiently form PtdIns[3,5]P_2, a new potential substrate for the *INP5* genes. It is intriguing to speculate that Inp52p, Inp53p or Inp54p may be specific for the PtdIns[3,5]P_2 isomer, while Inp51p exclusively works on PtdIns[4,5]P_2. High resolution HPLC studies of *in vivo* labeled inositol metabolites generated from hyperosmotically stressed *inp5* null strains may provide insights into the distinct roles of the *INP5* genes in yeast and mammalian cells.

The authors thank John McMillan, Daniel J. Lew, Joseph Heitman, John J. Moskow, Jeffrey S. Flick, Bryan D. Spiegelberg, John Connor and Jason Longchamps for technical advice and helpful discussions, and Sara Miller and Susan Hester for preparation of the electron micrographs. This work was supported by a Burroughs Wellcome Fund Career Development Award in the Biomedical Sciences, by funds from Merck Research Laboratories, by Research Grant HL-55672 from the National Heart, Lung, and Blood Institute (to J.D.Y.), by Predoctoral Traineeship GM07232 (to C.V.H.), and by Research Grant GM21841 from the National Institute of General Medical Sciences (to J.T.).

LITERATURE CITED

Attree, O., I. M. Olivos, I. Okabe, L. C. Bailey, D. L. Nelson *et al.*, 1992 The Lowe's oculocerebrorenal syndrome gene encodes a protein highly homologous to inositol polyphosphate-5-phosphatase. Nature **358:** 239–242.

Ausubel, F. M., R. Brent, R. E. Kingston, D. D. Moore, J. G. Seidman *et al.* (Editors), 1995 *Current Protocols in Molecular Biology*, John Wiley & Sons, Inc., New York.

Bansal, V. S., and P. W. Majerus, 1990 Phosphatidylinositol-derived precursors and signals. Ann. Rev. Cell Biol. **6:** 41–67.

Berridge, M. J., 1993 Inositol trisphosphate and calcium signaling. Nature **361:** 315–325.

Chowdhury, S. K. W. Smith and M. C. Gustin, 1992 Osmotic stress and the yeast cytoskeleton: phenotype-specific suppression of an actin mutation. J. Cell Biol. **118:** 561–571.

Cleves, A. E., P. J. Novick and V. A. Bankaitis, 1989 Mutations in the *SAC1* gene suppress defects in yeast Golgi and yeast actin function. J. Cell Biol. **109:** 2939–2950.

Communi, D., and C. Erneux, 1996 Identification of an active site cysteine residue in human type I Ins(1,4,5)P_3 5-phosphatase by chemical modification and site-directed mutagenesis. Biochem. J. **320:** 181–186.

Communi, D., R. Lecocq and C. Erneux, 1996 Arginine 343 and 350 are two active site residues involved in substrate binding by human type I d-*myo*-inositol 1,4,5-trisphosphate 5-phosphatase. J. Biol. Chem. **271:** 11676–11683.

Connolly, T. M., T. E. Bross and P. W. Majerus, 1985 Isolation of a phosphomonoesterase from human platelets that specifically hydrolyzes the 5-phosphate of inositol 1,4,5-trisphosphate. J. Biol. Chem. **260:** 7868–7874.

Damen, J. E., L. Liu, P. Rosten, R. K. Humphries, A. B. Jefferson *et al.*, 1996 The 145-kD protein induced to associate with Shc by multiple cytokines is an inositol tetraphosphate and phosphatidylinositol 3,4,5-trisphosphate 5-phosphatase. Proc. Natl. Acad. Sci. USA **93:** 1689–1693.

De Smedt, F., B. Verjans, P. Mailleux and C. Erneux, 1994 Cloning and expression of human brain type I inositol 1,4,5-trisphosphate 5-phosphatase. FEBS **347:** 69–72.

De Smedt, F., A. Bloom, X. Pesesse, S. N. Schiffman and C. Erneux, 1996 Post-translational modification of human brain type I inositol-1,4,5-trisphosphate 5-phosphatase by farnesylation. J. Biol. Chem. **271:** 10419–10424.

Dove, S. K., F. T. Cooke, M. R. Douglas, L. G. Sayers, P. J. Parker *et al.*, 1997 Osmotic stress activates phosphatidylinositol-3,5-bisphosphate synthesis. Nature **390:** 187–192.

Drayer, A. L., X. Pesesse, F. De Smedt, D. Communi, C. Moreau *et al.*, 1996 The family of inositol and phosphatidylinositol polyphosphate 5-phosphatases. Biochem. Soc. Trans. **24:** 1001–1005.

Flanagan, C. A., E. A. Schnieders, A. W. Emerick, R. Kunisawa, A. Admon *et al.*, 1993 Phosphatidylinositol 4-kinase: gene structure and requirement for yeast cell viability. Science **262:** 1444–1448.

Flick, J. S., and J. Thorner, 1993 Genetic and biochemical characterization of a phosphatidylinositol-specific phospholipase C in *Saccharomyces cerevisiae*. Mol. Cell. Biol. **13:** 5861–5876.

Guthrie, C., and G. R. Fink (Editors), 1991 *Guide to Yeast Genetics and Molecular Biology*. Academic Press, Inc., New York.

Harlan, J. E., P. J. Hajduk, H. S. Yoon and S. W. Fesik, 1994 Pleckstrin homology domains bind to phosphatidylinositol-4,5-bisphosphate. Nature **371:** 168–170.

Harlow, E., and W. Lane, 1988 *Antibodies: A Laboratory Manual*. Cold Spring Harbor Laboratory Press, Cold Spring Harbor, NY.

Hartwig, J. H., G. M. Bokoch, C. L. Carpenter, P. A. Janmey, L. A. Taylor *et al.*, 1995 Thrombin receptor ligation and activated Rac uncap actin filament barbed ends through phosphoinositide synthesis in permeabilized human platelets. Cell **82:** 643–653.

Hawkins, P. T., T. R. Jackson and L. R. Stephens, 1992 Platelet-derived growth factor stimulates synthesis of PtdIns(3,4,5)P_3 by activating a PtdIns(4,5)P_2 3-OH kinase. Nature **358:** 157–159.

Hay, J. C., P. L. Fisette, G. H. Jenkins, K. Fukami, T. Takenawa *et al.*, 1995 ATP-dependent inositide phosphorylation required for Ca^{2+}-activated secretion. Nature **374:** 173–177.

Hokin, L. E., 1985 Receptors and phosphoinositide-generated second messengers. Ann. Rev. Biochem. **54:** 205–235.

Irvine, R., 1992 Second messengers and Lowe syndrome. Nature Genetics **1:** 315–316.

Irvine, R. F., R. M. Moor, W. K. Pollock, P. M. Smith and K. A. Wreggett, 1988 Inositol phosphates: proliferation, metabolism and function. Philos. Trans. R. Soc. Lond. B. Biol. Sci. **320:** 281–298.

Jackson, S. P., S. M. Schoenwaelder, M. Matzaris, S. Brown and C. A. Mitchell, 1995 Phosphatidylinositol 3,4,5-trisphosphate is a substrate for the 75 kDa inositol polyphosphate 5-phosphatase and a novel 5-phosphatase which forms a complex with the p85/p110 form of phosphoinositide 3-kinase. EMBO J. **14:** 4490–4500.

Janmey, P. A., J. Lamb, P. G. Allen and P. T. Matsudaira, 1992 Phosphoinositide-binding peptides derived from the sequences of gelsolin and villin. J. Biol. Chem. **267:** 11818–11823.

Jefferson, A. B., and P. W. Majerus, 1995 Properties of Type II inositol polyphosphate 5-phosphatases. J. Biol. Chem. **270:** 9370–9377.

Jefferson, A. B., and P. W. Majerus, 1996 Mutation of the conserved domains of two inositol polyphosphate 5-phosphatases. Biochemistry. **35:** 7890–7894.

Jefferson, A. B., V. Auethavekiat, D. A. Pot, L. T. Williams and P. W. Majerus, 1997 Signaling inositol polyphosphate-5-phosphatase. J. Biol. Chem. **272:** 5983–5988.

Jones, J. S., and L. Prakash, 1990 Yeast *Saccharomyces cerevisiae* selectable markers in pUC18 polylinkers. Yeast **6:** 363–366.

Kearns, B. G., T. P. McGee, P. Mayinger, A. Gedvilaite, S. E. Phillips *et al.*, 1997 Essential role for diacylglycerol in protein transport from the yeast Golgi complex. Nature **387:** 101–105.

Kunz, J., R. Henriquez, U. Schneider, M. Deuter-Reinhard, N. R. Movva *et al.*, 1993 Target of rapamycin in yeast, TOR2, is an essential phosphatidylinositol kinase homolog required for G1 progression. Cell **73:** 585–596.

Laxminarayan, K. M., M. Matzaris, C. J. Speed and C. A. Mitchell, 1993 Purification and characterization of a 43-kDa membrane-associated inositol polyphosphate 5-phosphatase from human placenta. J. Biol. Chem. **268:** 4968–4974.

Laxminarayan, K. M., B. K. Chan, T. Tetaz, P. I. Bird and C. A. Mitchell, 1994 Characterization of a cDNA encoding the 43-kDa membrane-associated inositol-polyphosphate 5-phosphatase. J. Biol. Chem. **269:** 17305–17310.

Levin, D. E., and E. Bartlett-Heubusch, 1992 Mutants in the *S. Cerevisiae PKC1* gene display a cell cycle-specific osmotic stability defect. J. Cell Biol. **116:** 1221–1229.

Lioubin, M. N., P. A. Algate, S. Tsai, K. Carlberg, R. Aebersold *et al.*, 1996 $p150^{SHIP}$, a signal transduction molecule with inositol polyphosphate-5-phosphatase activity. Genes Dev. **10:** 1084–1095.

Luo, W.-J., and A. Chang, 1997 Novel genes involved in endosomal traffic in yeast revealed by suppression of a targeting-defective plasma membrane ATPase mutant. J. Cell Biol. **138:** 731–746.

Majerus, P. W., 1992 Inositol phosphate biochemistry. Ann. Rev. Biochem. **61:** 225–250.

Majerus, P. W., 1996 Inositols do it all. Genes Dev. **10:** 1051–1053.

Majerus, P. W., T. S. Ross, T. W. Cunningham, K. K. Caldwell, A. B. Jefferson *et al.*, 1990 Recent insights in phosphatidylinositol signaling. Cell **63:** 459–465.

Matzaris, M., S. P. Jackson, K. M. Laxminarayan, C. J. Speed and C. A. Mitchell, 1994 Identification and characterization of the phosphatidylinositol-(4,5)-bisphosphate 5-phosphatase in human platelets. J. Biol. Chem. **269:** 3397–3402.

Mayinger, P., V. A. Bankaitis and D. I. Meyer, 1995 Sac1p mediates the adenosine triphosphate transport into yeast endoplasmic reticulum that is required for protein translocation. J. Cell Biol. **131:** 1377–1386.

McLaughlin, M. M., S. Kumar, P. C. McDonnell, S. Van Horn, J. C. Lee *et al.*, 1996 Identification of mitogen-activated protein (MAP) kinase-activated protein kinase-3, a novel substrate of CSBP p38 MAP kinase. J. Biol. Chem. **271:** 8488–8492.

McPherson, P. S., A. J. Czernik, T. J. Chilcote, F. Onofri, F. Benfenati *et al.*, 1994a Interaction of Grb2 via its Src homology 3 domains with synaptic proteins including synapsin I. Proc. Natl. Acad. Sci. USA **91:** 6486–6490.

McPherson, P. S., K. Takei, S. L. Schmid and P. De Camilli, 1994b p145, a major Grb2-binding protein in brain, is co-localized with dynamin in nerve terminals where it undergoes activity-dependent dephosphorylation. J. Biol. Chem. **269:** 30132–30139.

McPherson, P. S., E. P. Garcia, V. I. Slepnev, C. David, X. Zhang *et al.*, 1996 A presynaptic inositol-5-phosphatase. Nature **379:** 353–357.

Mitchell, C. A., T. M. Connolly and P. W. Majerus, 1989 Identification and isolation of a 75-kDa inositol polyphosphate-5-phosphatase from human platelets. J. Biol. Chem. **264:** 8873–8877.

Mitchell, C. A., S. Brown, J. K. Campbell, A. D. Munday and C. J. Speed, 1996 Regulation of second messengers by the inositol polyphosphate 5-phosphatases. Biochem. Soc. Trans. **24:** 994–1000.

Novick, P., B. C. Osmond and D. Botstein, 1989 Suppressors of yeast actin mutations. Genetics **121:** 659–674.

Olivos-Glander, I. M., P. A. Janne and R. L. Nussbaum, 1995 The oculocerebrorenal syndrome gene product is a 105-kD protein localized to the Golgi complex. Am. J. Hum. Genet. **57:** 817–823.

Palmer, F. B. St. C., R. Theolis, Jr., H. W. Cook and D. M. Byers, 1994 Purification of two immunologically related phosphatidylinositol-(4,5)-bisphosphate phosphatases from bovine brain cytosol. J. Biol. Chem. **269:** 3403–3410.

Posas, F., A. Casamayor and J. Arino, 1993 The PPZ protein phosphatases are involved in the maintenance of osmotic stability of yeast cells. FEBS **318:** 282–286.

Rameh, L. E., C.-S. Chen and L. C. Cantley, 1995 Phosphatidylinositol $(3,4,5)P_3$ interacts with SH2 domains and modulates PI 3-kinase association with tyrosine-phosphorylated proteins. Cell **83:** 821–830.

Reed, R. H., J. A. Chudek, R. Foster and G. M. Gadd, 1987 Osmotic significance of glycerol accumulation in exponentially growing yeasts. Appl. Environ. Micro. **53:** 2119–2123.

Sikorski, R. S., and P. Hieter, 1989 A system of shuttle vectors and yeast host strains designed for efficient manipulation of DNA in *Saccharomyces cerevisiae*. Genetics **122:** 19–27.

Singh, A., and T. R. Manney, 1974 Genetic analysis of mutations affecting growth of *Saccharomyces cerevisiae* at low temperature. Genetics **77:** 651–659.

Srinivasan, S., M. Seaman, Y. Nemoto, L. Daniell, S. F. Suchy *et al.*, 1997 Disruption of three phosphatidylinositol polyphosphate 5-phosphatase genes from *S. cerevisiae* results in pleiotropic abnormalities of vacuole morphology, cell shape and osmohomeostasis. Eur. J. Cell Biol. **74:** 350–360.

Stack, J. H., D. B. DeWald, K. Takegawa and S. D. Emr, 1995 Vesicle-mediated protein transport: regulatory interactions between the Vps15 protein kinase and the Vps34 PtdIns 3-kinase essential for protein sorting to the vacuole in yeast. J. Cell Biol. **129:** 321–334.

Varela, J. C., C. van Beekvelt, R. J. Planta and W. H. Mager, 1992 Osmostress induced changes in yeast gene expression. Mol. Microbiol. **6:** 2183–2190.

Verjans, B., F. De Smedt, R. Lecocq, V. Vanweyenberg, C. Moreau *et al.*, 1994 Cloning and expression in *Escherichia coli* of a dog thyroid cDNA encoding a novel inositol 1,4,5-trisphosphate 5-phosphatase. Biochem. J. **300:** 85–90.

Vida, T. A., and S. D. Emr, 1995 A new vital stain for visualizing vacuolar membrane dynamics and endocytosis in yeast. J. Cell Biol. **128:** 779–792.

Whitters, E. A., A. E. Cleves, T. P. McGee, H. B. Skinner and V. A. Bankaitis, 1993 Sac1p is an integral membrane protein that influences the cellular requirement for phospholipid transfer protein function and inositol in yeast. J. Cell Biol. **122:** 79–94.

Woscholski, R., M. D. Waterfield and P. J. Parker, 1995 Purification and biochemical characterization of a mammalian phosphatidylinositol 3,4,5-trisphosphate 5-phosphatase. J. Biol. Chem. **270:** 31001–31007.

York, J. D., and P. W. Majerus, 1994 Nuclear phosphatidylinositols decrease during S-phase of the cell cycle in HeLa cells. J. Biol. Chem. **269:** 7847–7850.

Yoshida, S., Y. Ohya, M. Goebl, A. Nakano and Y. Anraku, 1994 A novel gene, *STT4*, encodes a phosphatidylinositol 4-kinase in the *PKC1* protein kinase pathway of *Saccharomyces cerevisiae*. J. Biol. Chem. **269:** 1166–1172.

Zhang, F. L., and P. J. Casey, 1996 Protein prenylation: molecular mechanisms and functional consequences. Annu. Rev. Biochem. **65:** 241–269.

Zhou, M.-M., K. S. Ravichandran, E. T. Olejniczak, A. M. Petros, R. P. Meadows *et al.*, 1995 Structure and ligand recognition of the phosphotyrosine binding domain of Shc. Nature **378:** 584–592.

Communicating editor: M. Johnston